designs

MDPI

Article

A Numerical Thermal Analysis of a Battery Pack in an Electric Motorbike Application

Mohammad Shahjalal [1], Tamanna Shams [2], Sadat Bin Hossain [3], Probir Kumar Roy [3], Arafat Alam Jion [3], Mominul Ahsan [4,*], Jahedul Islam Chowdhury [5], Md Rishad Ahmed [6], Syed Bahauddin Alam [7] and Julfikar Haider [8]

1 Department of WMG, University of Warwick, Coventry CV4 7AL, UK; mohammadshahjalal15@yahoo.com
2 Department of Physics, University of Dhaka, Dhaka 1000, Bangladesh; tamanna.shapla@yahoo.com
3 Department of Mechanical Engineering, Chittagong University of Engineering and Technology (CUET), Chattogram 4349, Bangladesh; sbh.pranto.24@gmail.com (S.B.H.); probirroy1702085@gmail.com (P.K.R.); arafatjion11803050@gmail.com (A.A.J.)
4 Department of Computer Science, University of York, Deramore Lane, York YO10 5GH, UK
5 School of Aerospace, Transport and Manufacturing, Cranfield University, Bedford MK43 0AL, UK; j.chowdhury@cranfield.ac.uk
6 Department of Electrical and Electronic Engineering, University Park Campus, University of Nottingham, Nottingham NG7 2RD, UK; rishad.ahmed@nottingham.ac.uk
7 Nuclear Engineering and Radiation Science, Missouri University of Science and Technology, Rolla, MO 65409, USA; alams@mst.edu
8 Department of Engineering, Manchester Metropolitan University, John Dalton Building, Chester Street, Manchester M1 5GD, UK; j.haider@mmu.ac.uk
* Correspondence: md.ahsan2@mail.dcu.ie

Citation: Shahjalal, M.; Shams, T.; Hossain, S.B.; Roy, P.K.; Jion, A.A.; Ahsan, M.; Chowdhury, J.I.; Ahmed, M.R.; Alam, S.B.; Haider, J. A Numerical Thermal Analysis of a Battery Pack in an Electric Motorbike Application. *Designs* **2022**, *6*, 60. https://doi.org/10.3390/designs6040060

Academic Editor: Quanqing Yu

Received: 9 May 2022
Accepted: 20 June 2022
Published: 22 June 2022

Abstract: Today, electric driven motorbikes (e-motorbikes) are facing multiple safety, functionality and operating challenges, particularly in hot climatic conditions. One of them is the increasing demand for efficient battery cooling to avoid the potential thermal stability concerns due to extreme temperatures and the conventional plastic enclosure of the battery pack. A reliable and efficient thermal design can be formulated by accommodating the battery within an appropriate battery housing supported by a cooling configuration. The proposed design includes a battery pack housing made of high conductive materials, such as copper (Cu) and aluminum (Al), with an adequate liquid cooling system. This study first proposes a potted cooling structure for the e-motorbike battery and numerical studies are carried out for a 72 V, 42 Ah battery pack for different ambient temperatures, casing materials, discharge rates, coolant types, and coolant temperatures. Results reveal that up to 53 °C is achievable with only the Cu battery housing material. Further temperature reduction is possible with the help of a liquid cooling system, and in this case, with the use of coolant temperature of 20 °C, the battery temperature can be maintained within 28 °C. The analysis also suggests that the proposed cooling system can keep a safe battery temperature up to a 5C rate. The design was also validated for different accelerated driving scenarios. The proposed conceptual design could be exploited in future e-motorbike battery cooling for optimum thermal stability.

Keywords: battery pack; electric motorbike; battery housing; heat transfer; FEA

1. Introduction

To reduce carbon emissions, most countries are focusing on designing and developing energy efficient and environmentally friendly transportation systems. As a means of short-range transportation, electric motorbikes (e-motorbikes) have already gained immense popularity due to their advantages of low noise, convenience, and less pollution. Currently, e-motorbike manufacturers exploit commercially available Li-ion batteries instead of lead–acid batteries to gain the advantages of high-power density (4–5 times higher than a typical lead-acid battery) [1–3]. Battery health is a serious concern to vehicle manufacturers. Fire

safety is one of the important issues, particularly for large assembly battery packs [4]. A case study on achieving a high discharge current of 184 A is reported in [5]. To satisfy high power demand, a new Al-ion type battery has been introduced [6]. Temperature issues have been modelled for lithium-titanate batteries at an increased cycling rate [7]. More thermal studies have been carried out; for example, preheating is employed to prevent lithium deposition [8]. One work found a link to cell behavior under different ambient temperatures [9]. However, these previous studies are more linked to batteries used in electric vehicles (EV) and do not deal thoroughly with issues such as battery operation in e-motorbikes in high climatic conditions. During the charging or discharging process, the battery will experience heat due to an internal resistance effect and entropic effect (exothermic reactions inside the battery). The generated heat will lead to battery temperature rise and large temperature gradients across the battery pack, resulting in capacity fade [10], power fade [11], thermal runaway, and varied forms of battery ageing and degradation [12,13]. Batteries are currently configured in e-motorbikes by placing them in a plastic case, which acts like an insulator. The external air cannot pass to the battery pack. Thus, battery safety is the biggest concern in the context of hot climatic conditions present in Middle East countries, California in the United States, Central and Southeast China, and Japan and other Southeast Asian countries, where, usually, the ambient temperature goes up to 45 °C during summer. The permissible temperature difference across the pack is below 5 °C [14–16]. Therefore, an efficient thermal management strategy needs to be formulated to ensure the battery's safety and reliability in extreme ambient temperatures.

Several battery cooling concepts exist in the market, including air cooling and liquid cooling, and both have their relative advantages and disadvantages [17,18]. Air cooling is a cost-effective and generally less efficient method in achieving uniform temperature across the battery pack. Air cooling is often problematic for heat removal from batteries, particularly under abusive conditions [19]. A hybrid thermal management system (TMS) has been proposed for investigating the thermal characteristics of Lithium-ion (Li-ion) batteries and cell-embedded fin heat sink (CHS) to improve the cooling and temperature consistency of a lithium-titanite (LTO) cell in high-current discharging [17]. Their experiments showed that an inlet velocity of 3 m/s preserves the CHS in a safe temperature zone that reduces the fan power consumption by 50%. In contrast, liquid cooling is more efficient compared to air cooling, although high cost and maintenance associated with it are a concern [20]. The work presented in [18] has performed analysis on thermal management systems considering air type and liquid type to enhance energy efficiency for a Li-ion battery with a 48 V module and 12 prismatic-shape Nickel Manganese Cobalt Oxide (NMC). To test the module, an experimental test bench was built at room temperature without having any cooling system. A U-type parallel air cooling and a new indirect liquid cooling system were designed and investigated for a 2C discharge process. The results showed a lower module temperature and better temperature uniformity where power consumption was achieved around 0.5 W, and the average temperature of the hottest battery cell was around 3 °C lower than the air-cooled module. Karimi et al. [21] have proposed an optimal thermal management system (TMS) employing a heat pipe cooling system (HPCS) to extend the end of life (EoL) of a Li-ion capacitor (LiC). Liquid-cooled TMS (LCTMS) was considered to investigate the effect of temperature on LiC capacity fade. The results showed that HPCS controlled the temperature evolution of the cell during a 150 A charge/discharge current rate. Furthermore, the top surface temperature of the cell was reduced by 11.7% using the HPCS. In addition, the lifetime of the LiC was extended by 51.7% and 16.5%, whereas the temperature of the cell was kept at around 32.5 °C and 48.8 °C, respectively. However, the study was developed based on a smart grid application rather than an e-bike.

So far, no detailed research work is found regarding the cooling system for an e-motorbike battery. A conventional plastic battery housing will be problematic, particularly dealing with the issues, for instance, of lack of temperature uniformity across the pack and reducing the maximum operating battery temperature under hot climatic conditions. Battery housing material is an important element in battery enclosures and thus can be

an influential factor in battery thermal management for e-bike applications. The most widely used battery enclosure material is plastic, which is considered to be a material with poor thermal conductivity, making it unsuitable for high thermal load management. During the acceleration phase, the high thermal load that appears in an e-bike needs to be managed safely and efficiently. The proposed research work focuses on a comparative study of various battery housing materials on thermal performance of the battery pack to identify which battery housing material can manage a high thermal load. The two major contributions of this paper are to provide a basis for the selection of battery housing material for the thermal management in hot climatic conditions and to demonstrate that the effect of high ambient temperature on overall battery pack performance can be minimised with the use of an appropriate coolant.

In this work, a numerical model is established for simulating the thermal behaviour of an e-bike battery pack for various battery housing materials under various discharge rates. The effect of ambient temperature is also studied, and the design issues are also highlighted.

2. Methodology and Simulation

This section explains the simulation details regarding the battery pack's configuration, the material of the battery and structural details, simulation set up and boundary conditions, and numerical evaluation of the battery housing materials and coolant flow.

2.1. Battery Pack Configuration

The battery pack used in the e-motorbike consists of cells in a series of parallel connection. In order to investigate inhomogeneous cell behaviour within the battery system, it is necessary to consider all factors that are leading to different cell loads. An exploded view of the battery pack is shown in Figure 1. Battery cells are connected using a nickel strip. The battery pack is usually enclosed by molded plastic. Since plastic is not a good thermal conductor, the temperature of the battery pack will increase significantly. To investigate the impact of battery housing materials on temperature distribution in the battery pack, two battery housing materials (Al and Cu) will be studied.

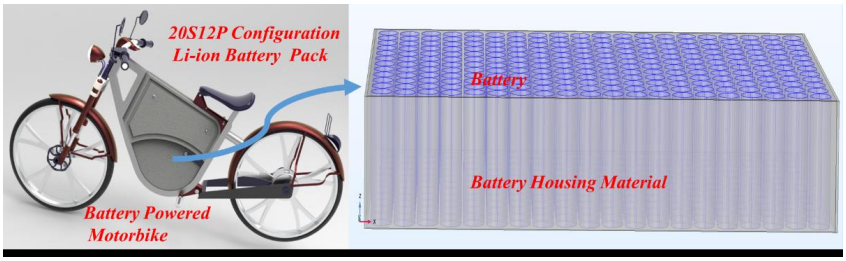

(**a**)

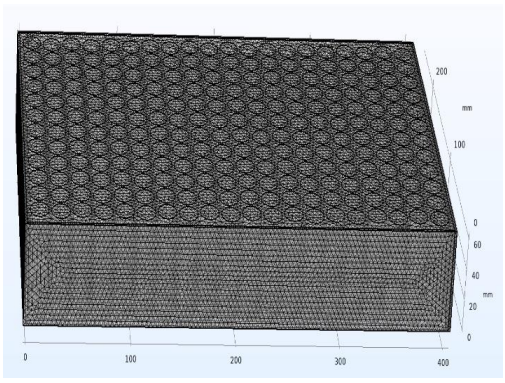

(**b**)

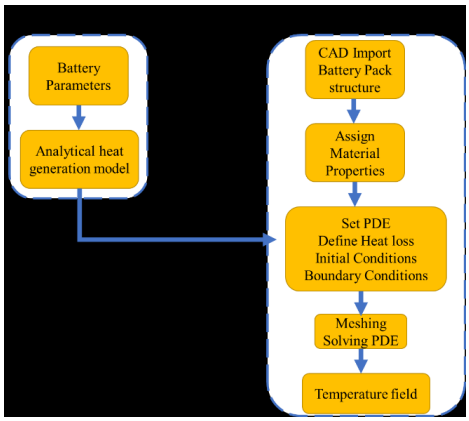

(**c**)

Figure 1. (**a**) Typical configuration of 2.8 kW electric motorbike containing 72 V 43 Ah battery pack and (**b**) meshed model of the studied battery pack and (**c**) thermal model set up.

2.2. Battery Thermal Model

The first step to establish the thermal model is to estimate the heat generation. Due to battery loading either in discharge or charge mode, heat generation is inevitable in the battery. Two sources of heat are very common. These include irreversible heat from the cell's internal resistance and reversible heat contributed by entropy change. This work has considered the irreversible heat source only. The battery studied had a high C rate, ranging from 1C to 5C. As entropic heating has a negligible impact at this high C rate, this term for estimating heat losses in the battery has not been considered. The overall generated heat can be obtained [22,23] as follows:

$$Q_{gen} = Q_{irr} + Q_{rev} = I(U_{ocv} - U_{batt}) - IT\frac{\partial U_{ocv}}{\partial T} \quad (1)$$

where Q_{gen} is the total heat generation rate of the battery cell, and Q_{irr} and Q_{rev} are the irreversible heat and reversible heat, respectively. I is the charge/discharge current of the battery cell. U_{ocv} is the open-circuit voltage, and U_{batt} is the battery voltage. T is the battery temperature, and $\partial U_{ocv}/\partial T$ is the temperature coefficient of open-circuit voltage. During the discharge process, the following formula can be obtained:

$$U_{batt} = U_{ocv} - IR \quad (2)$$

where R is the equivalent internal resistance, including the ohmic resistance and the polarisation equivalent resistance. By combining U_{batt} into Equation (1), the following equation can be obtained:

$$Q_{gen} = I^2R \quad (3)$$

2.3. FEA Model Development

The battery pack studied in this paper is taken from an e-motorbike application, as shown in Figure 1a. The mesh model of the studied battery pack is shown in Figure 1b. The thermal model set up is illustrated in Figure 1c. Since the number of degrees of freedom determines the memory requirement and the processing time, it is important to avoid the out-of-memory error. Increasing mesh size can decrease the need of high memory. Coarser mesh is chosen in this work to reduce the high computational load and the high memory requirement. The chosen battery pack consists of 240 cylindrical cells with a rated specification of 72 V 42 Ah capacity. The e-motorbike draws power from a 72 V Li-ion battery pack. The resultant battery pack takes a 20S12P configuration. To achieve a voltage rating of 72 V, 20 cells are configured in a series, and 12 strings (each string contains 20 cells) with a current rating of 42 A are connected in parallel. The cell used in this simulation is taken from commercial Panasonic cell [24] (Panasonic NCR18650B, Japan), with an internal resistance of 38 mΩ. The specifications of the batteries used in the battery pack are listed in Table 1.

As mentioned earlier, batteries are very sensitive to their operating temperature. Since batteries stay close to each other in a compact battery housing, heat generation and thermal crosstalk are serious concerns to be considered at the early design stage. Heat generation is inevitably high while the e-motorbike undergoes an extreme acceleration phase. The high discharge rate is thought to be a contributing factor to battery heat generation and thus, if such a high amount of heat is left untreated, the result can be battery failures, causing thermal runaway; in turn, a substantial amount of battery degradation and lifetime reduction will happen. The temperature of the battery has an impact on the design of the battery pack and reduction of temperature is dependent on the relevant cooling strategy to be chosen. For example, a key design index can start from the choice of a cooling strategy to the cooling material. In operation of the battery, such as in charge/discharge load profiles, losses are going to be introduced due to the battery's electrical characteristics and the thermodynamics of the battery's chemistry. Therefore, accurate thermal design is of the utmost importance and special efforts need to be invested for achieving a safe operating

thermal envelope. The efficient way of heat extraction of the battery pack in an e-motorbike is of concern at the design level, and it is therefore modelled by the energy conservation outlined in the heat transfer module in COMSOL.

Table 1. Specifications of 3.2 Ah battery [25].

Battery Specifications	Values
Diameter (mm)	18
Height (mm)	65
Weight (g)	45
Chemistry	Nickel/Cobalt/Rechargeable
Maximum Charging Voltage	4.2
Nominal Voltage (V)	3.7
Minimum Cut-off Voltage (V)	2.5
Maximum Capacity (mAh)	3350
Nominal Capacity (mAh)	3200
Internal Resistance (mΩ)	38
Battery Pack Configuration	20S12P
Working temperature range (°C)	Charge: 0 to +45 Discharge: −20 to +60

The general thermal behaviour of the battery due to the heat generated either during charge or discharge operating mode can be explained by the heat Equation (4) [26,27], which means that the temperature of the battery is a function of power loss density.

$$k\left(\frac{\partial^2 T}{\partial x^2}+\frac{\partial^2 T}{\partial y^2}+\frac{\partial^2 T}{\partial z^2}\right)+Q=\rho c_p\frac{\partial T}{\partial t} \tag{4}$$

where, for the battery, c_p is the battery specific heat capacity, ρ is the density, k is the thermal conductivity, T is the battery temperature, which is a function of space and time, and Q is the heat generation rate.

For the sake of simplicity, only Joule heating is considered in this work. The thermal behaviour of the battery module is determined here by solving the 3D partial-differential heat transfer equations. The diffusion–convection governing energy equation is used to solve the temperature field problem, as expressed in Equation (4). The established thermal model is capable of identifying the localized hotspot, maximum temperature, and temperature elevations above the ambient on the battery module in an enclosed system.

Battery housing material is an important factor in thermal management of the battery pack, where cells are accommodated in a dense and compact configuration. A finite, element-based 3D thermal model is established to determine the steady-state temperatures reached by the potted/housed battery pack and to investigate the use of different housing materials for reducing temperature. The simulations considered the battery, battery tab connection, and battery casing Al/Cu structure.

The purpose of the established finite element analysis (FEA) thermal model is to study the impact of battery housing material on the total temperature distribution of the battery pack. Volumetric heat is applied in each battery cell. The constant temperature boundary conditions are applied at the bottom of the battery housing material. For the sake of simplicity, the battery housing structure is kept adiabatic in the lateral sides, and therefore, all the generated heat is dissipated through the air to the battery enclosure structure casing via conduction and the casing to the environment via convection. Since the battery enclosure structure is located outside the e-motorbike and exposed to the surrounding air, the heat transfer mechanism from the casing to the environment via convection can be treated as convective thermal boundary conditions. To emulate convective behaviour, convective boundary conditions are applied to all of the surfaces of the can structure. In this model, convective boundary conditions are set to h = 5.0 $W{\cdot}m^{-2}{\cdot}K^{-1}$, representing free air convection. The ambient temperatures of the battery enclosure are set to 5 °C, 15 °C,

35 °C, and 45 °C to simulate a wide range of temperature variations in different parts of the world. The rationale for choosing Al and Cu as the battery housing materials is mainly for two reasons. One is high thermal conductivity, and the second is sustainability to operate at temperatures up to 100 °C. After meshing the studied battery pack, the constructed FEA thermal model was solved in the COMSOL Multiphysics three-dimensional (3D) FEA software using the static thermal solver. Thermo-physical properties of the battery and the casing materials are listed in Table 2.

Table 2. Thermo-physical properties of Battery and casing materials [27].

Material	Density ρ (kg·m^{-3})	Specific Heat Capacity c_p(J·kg^{-1}·K^{-1})	Thermal Conductivity k (W·m^{-1}·K^{-1})
Battery	2500	1200	4
Al	2719	871	202
Cu	8960	385	400

2.4. Mesh Independence Test

The mesh size is an important parameter in thermal simulation. This section describes the impact of different mesh sizes on thermal calculation accuracy. The mesh size includes fine, normal, coarse, coarser, and extra coarse. In all cases, the same discharge rate 3C condition is applied and the ambient temperature of the battery is set to 45 °C. Figure 2 shows that the temperature estimated under different mesh sizes does not vary too much and remains within an acceptable level of difference. The difference in results is only 0.8% when the grid number increases from 46,765 to 1,162,082. Therefore, the grid number of 46,765 is chosen in this work to accelerate simulation.

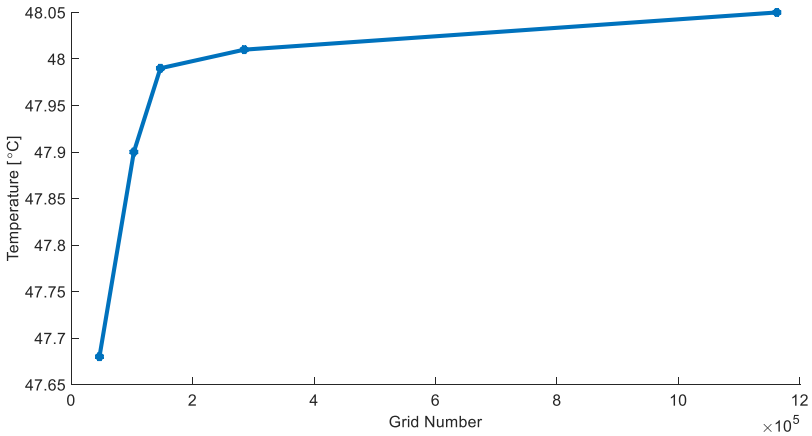

Figure 2. Mesh independence test showing variation in temperature with the grid number.

3. Results and Discussion

Battery operating temperature is critical in terms of battery safety, lifetime, and performance. Thermal management of the Li-ion battery draws serious attention, particularly in hot climatic conditions. Two factors, such as battery housing material and operating ambient temperature, might have a significant impact on the temperature distribution and cooling performance. This section explains the results obtained for a potted battery pack at different ambient temperatures and at different discharge rates.

3.1. Effect of Ambient Temperature

Since the ambient temperature affects the total temperature distribution of the battery pack, the variation in ambient temperature is studied in this section. To understand the effect of ambient temperature on the battery pack, several simulations are performed at 5 °C, 15 °C, 35 °C, and 45 °C ambient temperatures. The volumetric power losses

in each battery are applied during the discharge rate of 0.5C, 1C, 3C, and 5C [28]. To understand the thermal behaviour of the battery pack while the battery is housed in plastic, a simulation is set up with the plastic battery housing material at a discharge rate of 2C, and the ambient temperature is considered 5 °C. The temperature distribution of the battery pack is presented in Figure 3. It is observed that the battery operating temperature goes up high and it reaches up to 60 °C. This temperature rise can be attributed to the fact that low thermal conductivity plastic is not a good candidate as a battery housing material.

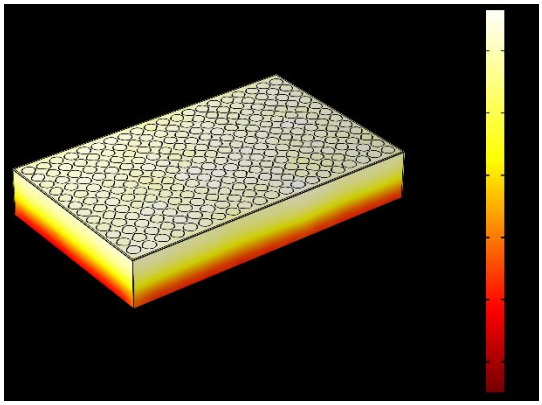

Figure 3. Temperature contours of the entire battery pack in plastic (acrylic) housing at 2C discharge rate while ambient temperature of 5 °C is considered.

To minimise the temperature of the battery pack, a high thermal conductive battery casing material such as Al and Cu can be used. Figure 4 shows the maximum temperature rises of the battery pack at ambient temperature of 5 °C at the end of different discharge rates. The temperature rise is observed at an increasing ambient temperature. It is evident that the higher the ambient temperature, the greater the temperature elevation. The temperature elevation can be reduced if Cu is chosen as the battery housing material compared to Al. Temperature elevation can be reduced significantly due to the high thermal conductivity of Cu.

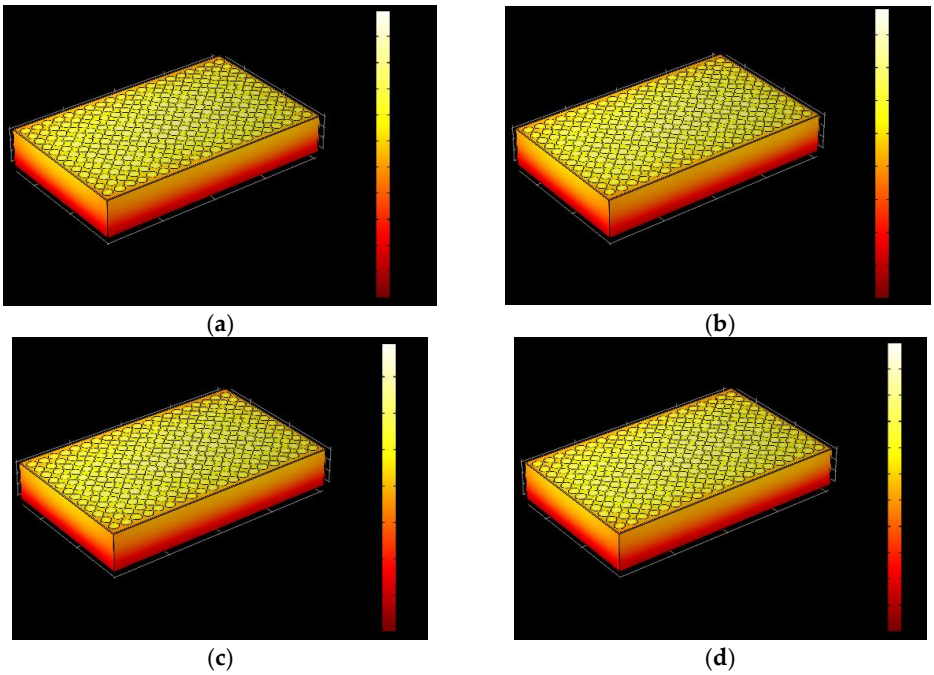

Figure 4. Temperature contours of the entire battery pack in Al housing with different C rates (**a**) 0.5C (**b**) 1C (**c**) 3C (**d**) 5C while ambient temperature of 5 °C is considered.

The temperature contours obtained from the FEA thermal simulations at 0.5C, 1C, 3C, and 5C discharge rate while operating at 45 °C ambient temperature are shown in Figure 5. It is observed that there is a great impact of operating ambient temperature on the performance of the battery and battery housing, and it is observed that as the ambient temperatures increases between 5 °C to 45 °C for a particular discharge rate of 0.5C, 1C, 3C, and 5C, the temperature contour values are also increased. The general temperature elevation patterns are the same, showing greater temperatures at the ambient temperature of 45 °C. The temperatures vary with the ambient temperature boundary condition, but the overall temperature distribution shows identical patterns in almost all the cases. The temperature elevation is higher due to varying elevated operating ambient temperature conditions.

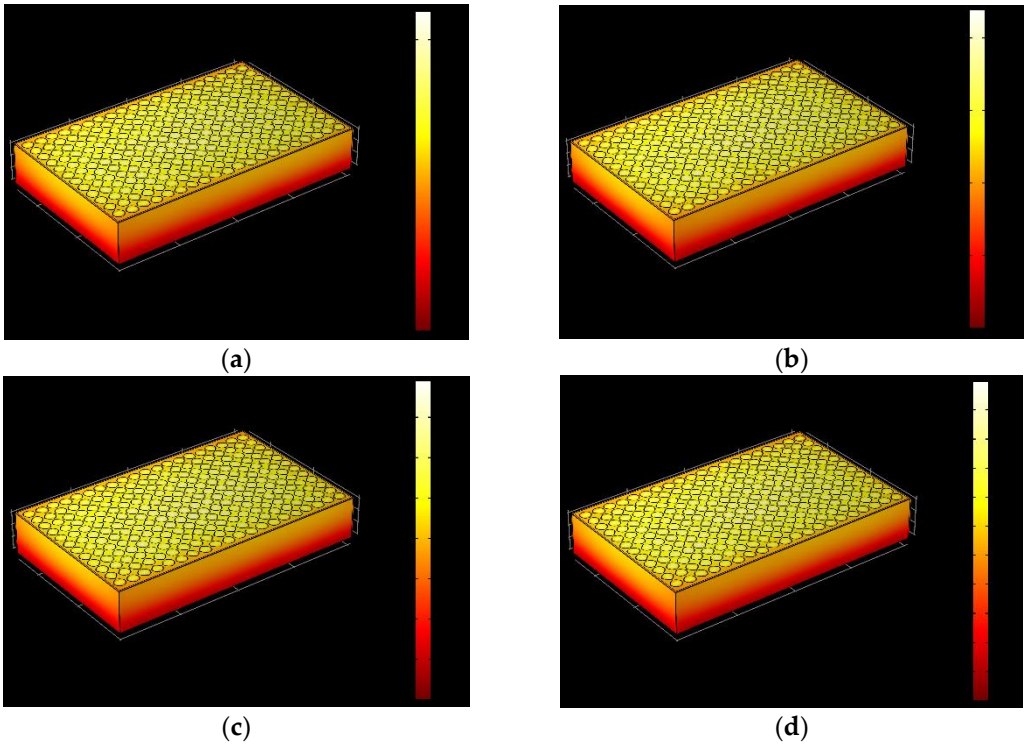

Figure 5. Temperature contours of the entire battery pack in Al housing with different C rates (**a**) 0.5C (**b**) 1C (**c**) 3C (**d**) 5C while ambient temperature of 45 °C is considered.

The temperature contours at 0.5C, 1C, 3C, and 5C discharge rates while operating at 45 °C ambient temperature are illustrated in Figure 6. It is seen that as the battery housing material changes from Al to Cu, there is a reduction in the temperature values as well. Figure 7 describes the maximum temperature elevations of battery packs fitted with Al and Cu battery housings under different ambient temperatures at varied C rates. Table 3 describes predicted battery temperatures at varied C rates with different housing materials.

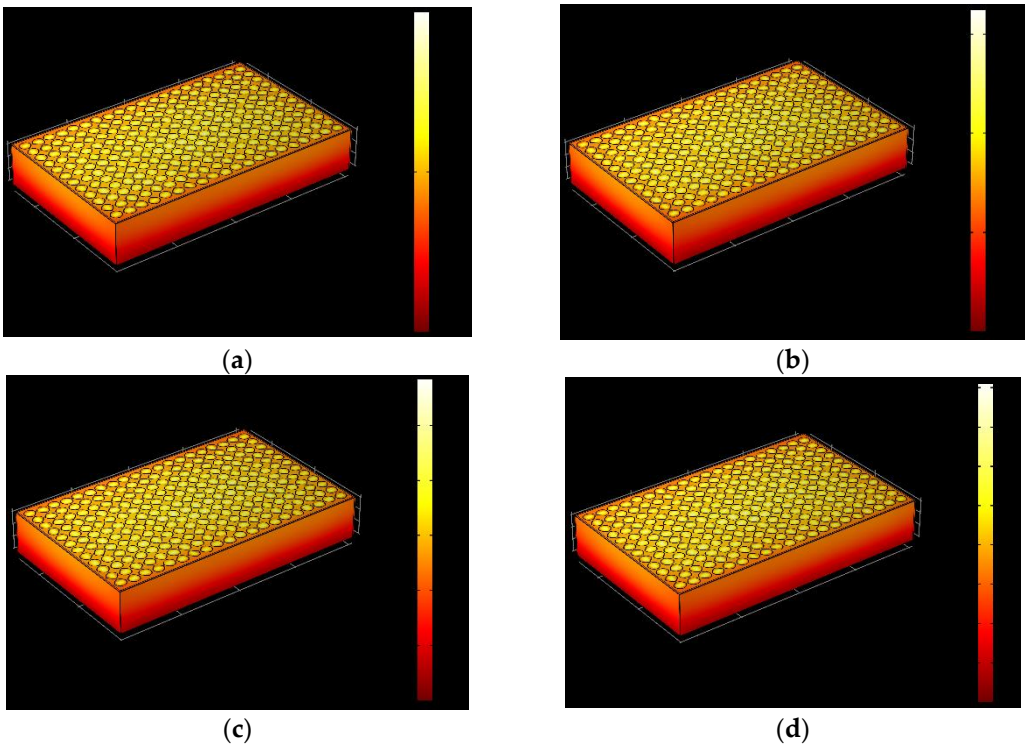

Figure 6. Temperature contours of the entire battery pack in Cu housing with different C rates (**a**) 0.5C (**b**) 1C (**c**) 3C (**d**) 5C while ambient temperature of 45 °C is considered.

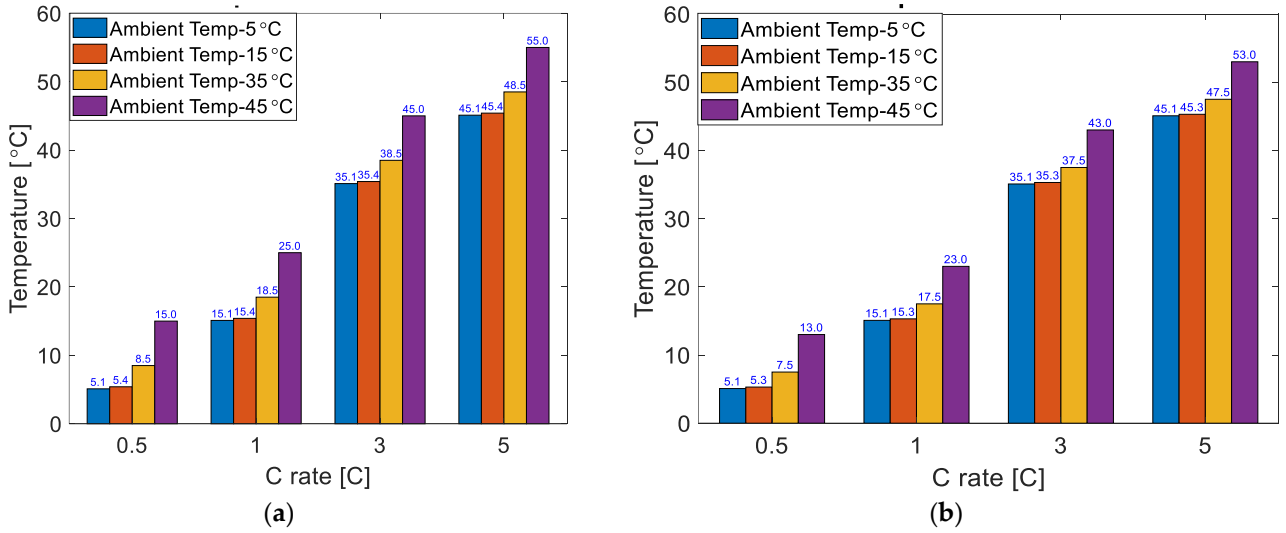

Figure 7. Maximum temperature elevations of battery pack implemented with (**a**) Al battery housing and (**b**) Cu battery housing under different ambient temperatures at varied C rates.

Table 3. Predicted Battery Temperature at varied C rates under different housing materials.

Ambient Temperature (°C)	Al Housing, Predicted Temperature (°C) at Different Discharge Rates				Cu Housing, Predicted Temperature (°C) at Different Discharge Rates			
	0.5C	1C	3C	5C	0.5C	1C	3C	5C
5	5.1	5.4	8.5	15	5.08	5.3	7.5	13
15	15.1	15.4	18.5	25	15.08	15.3	17.5	23
35	35.1	35.4	38.5	45	35.08	35.3	37.5	43
45	45.1	45.4	48.5	55	45.08	45.3	47.5	53

As the discharge rate increases from 0.5C to 1C, 3C, and 5C, the operating temperature increases. The temperature contour pattern observed is that increased discharge rates contribute to high heat loss and thus result in increased temperature. Again, the general temperature contour patterns are almost identical, similar to the results obtained from Al housing. The prime reason is thought be that increased discharge rate results in increased current going through the battery and joule heating due to the cell's internal resistance. The effect of discharge C rate is observed highest at the 5C rate compared to the other discharge C rates. At the 5C rate, the current is five times higher than at the 1C rate. Thus, the heat generation rate is five times higher than the 1C rate. The increase in ambient temperature boundary condition increases the temperature contour but produces almost the same trend in all cases. At a low ambient temperature, batteries exhibit high internal resistance, whereas at high ambient temperatures, batteries exhibit low internal resistance. The increase in ambient temperature accelerates the chemical reaction inside the battery, which accelerates battery fluid evaporation, resulting in damage of the internal structure and corrosion. The unwanted chemical reaction rate also goes up. Ultimately, the increased ambient temperature can accelerate the battery's failure, which can shorten the battery's life.

The findings reveal that Cu housing can reduce battery temperature from 55 °C (Al housing) to 53 °C. However, Cu housing is still not capable of achieving the battery temperature within a safe range (e.g., 15~40 °C). Therefore, an additional cooling strategy needs to be employed if battery temperature is to be maintained within a safe limit at 5C discharge conditions. To achieve this, coolant of varying temperatures can be employed, and appropriate liquid cooling needs to be configured at the bottom of the pack.

3.2. Effect of Coolant Temperature

As mentioned above, the battery operating temperature can rise up to 75 °C at the ambient boundary temperature of 45 °C. To keep the battery temperature in a safe window, a further simulation was conducted to study the effect of coolant temperature. The different coolant temperatures are 5 °C, 10 °C, 15 °C, and 20 °C. The fixed temperature boundary condition is applied at the bottom of the battery housing case material. The surrounding battery housing side wall temperature was set to 45 °C. The power losses in each battery are applied during discharge rates of 0.5C, 1C, 3C, and 5C. The water/glycol (50% + 50%) is used as a coolant and the representative heat transfer coefficient of h = 5000 $W \cdot m^{-2} \cdot K^{-1}$ for liquid cooling is applied. Figure 8 shows the temperature contours of the battery pack at different discharge rates with the applied cooling boundary condition of T_coolant = 20 °C. Under these conditions, the temperature is reduced for all discharge rates. As seen from the figure, even at the 5C discharge condition, the elevated battery temperature is 28 °C. It is observed that the impact of coolant temperature is significant. Battery operating temperature can be reduced to a tolerable thermal limit. The findings revealed that high thermal conductivity battery casing material needs to be used for a battery enclosure. In addition, external liquid-cooled thermal management needs to be employed while the battery is operated at a high discharge rate and in harsh ambient conditions. The temperature elevations at the discharge rates of 0.5C, 1C, 3C, and 5C while operating at 45 °C ambient temperature are illustrated in Figure 9. It is seen that as the liquid cooling is employed in the battery, there is a reduction in the temperature values as well.

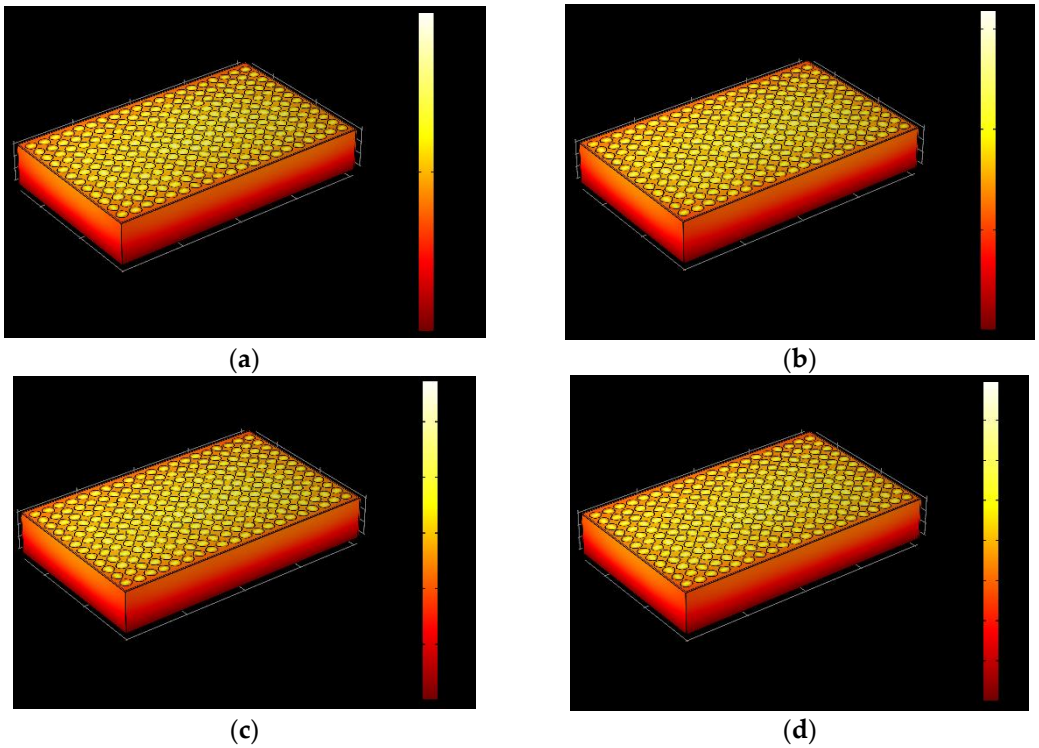

Figure 8. Temperature contours of the entire battery pack in Cu housing while coolant temperature is 20 °C with different C rates (**a**) 0.5C (**b**) 1C (**c**) 3C (**d**) 5C operating at 45 °C ambient temperature.

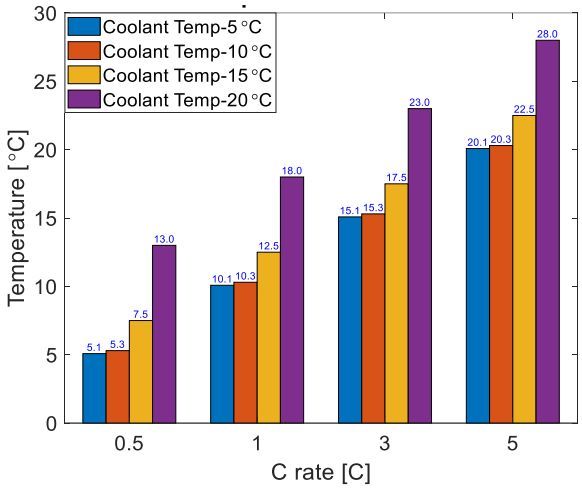

Figure 9. Maximum temperature elevations of battery pack fitted with Cu battery housing under different coolant temperatures at varied C rates operating at 45 °C ambient temperature.

3.3. Effect of Coolant Types

Battery temperature is critical to prevent battery degradation and thermal runaway. Since the battery is exposed to either charging or discharging, heat generation is inevitable. Therefore, appropriate thermal management is of major significance to keep the battery temperature within a safe operating limit. Thermal safety not only elevates the e-motorbike's reliability but also lessens the thermal failure of the battery pack. Liquid- cooled thermal management offers superior cooling performance. However, the choice of coolant must be taken into consideration to customize the liquid-cooled battery thermal management. Numerical modelling is a relatively suitable method to study the thermal distribution of the battery pack by comparison with experimental tests, which are not only costly but also time consuming. A numerical case study is established to predict the effects of coolant type

in battery temperature distribution. Two types of coolant have been considered in the work. These include dielectric mineral oil and water/glycol (50% + 50%). Coolant types that have high thermal conductivity, good specific heat capacity, and low viscosity are expected to enhance the thermal performance. The reason for choosing mineral oil as coolant is due to it not conducting an electric charge, which is important for battery applications. On the other hand, water/glycol is better than water alone due to its lower specific heat and freezing point. Furthermore, during summer, the water/glycol acts as coolant, whereas during winter it acts as an antifreeze. The thermal properties of each coolant material are listed in Table 4. The C-rate is varied from 0.5C to 5C. The study uses the equivalent heat transfer coefficient resulting from the flow rate of coolant. The coolant velocity is varied from 0.5 ms^{-1} to 3 ms^{-1}.

Table 4. Thermo-physical properties of coolant materials [29].

Material	Mineral Oil	Water/Glycol
Density ρ $\left(kg{\cdot}m^{-3}\right)$	924.1	1069
Specific heat capacity c_p $\left(J{\cdot}kg^{-1}{\cdot}K^{-1}\right)$	1900	3323
Thermal Conductivity k $\left(W{\cdot}m^{-1}{\cdot}K^{-1}\right)$	0.13	0.3892
Kinematic Viscosity m^2/s	5.6×10^{-5}	2.58×10^{-6}

A liquid cold plate is employed at the bottom of the battery pack. In order to establish an accurate numerical thermal model, estimation of an equivalent heat transfer coefficient (*htc*) is necessary. Based on the previous study [30], an equivalent heat transfer coefficient can be estimated for liquid cold plate cooling.

From the following expression, dimensionless Nusselt number can be calculated as

$$Nu = 0.023\ Re^{0.8} Pr^{0.4} \tag{5}$$

where Re is the Reynold Number and Pr is the Prandtl Number. The equivalent heat transfer coefficient can be estimated as

$$htc = \frac{Nu \times k}{D_h} \tag{6}$$

where k is the thermal conductivity of the cooling liquid and D_h is the hydraulic diameter.

In order to calculate the heat transfer coefficient, the fluid flow rate, tube diameter, and fluid thermo-physical properties were taken into account. The cold plate has a base size of 400 mm × 200 mm × 16 mm with an inlet diameter of 7 mm. Figure 10 presents a design of the proposed liquid cold plate. Specifications of the liquid cold plate are listed in Table 5.

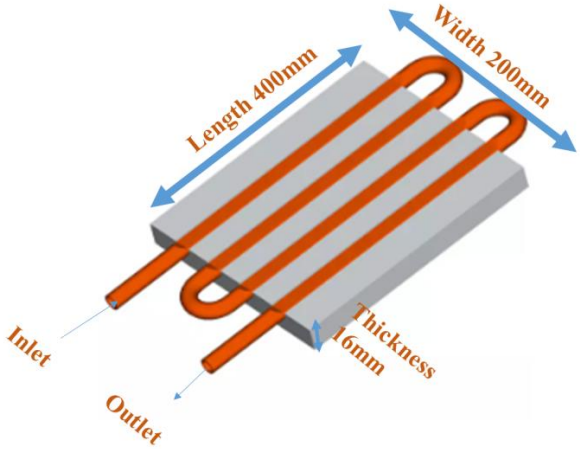

Figure 10. Proposed liquid cold plate for e-bike battery cooling.

Table 5. Specifications of the liquid cold plate.

Parameters	Values
Liquid cold plate size	400 mm × 200 mm × 16 mm
Maximum Diameter of the outer channel (mm)	9 mm
Channel pass	4
Working liquid	45
Channel	Cu
Working coolant temperature range (°C)	5–20

Battery temperature predicted at varied C rates under various coolants is listed in Table 6. Figure 11 demonstrates the temperature profiles under various charging/discharging rates, ranging from 0.5C to 5C. It is demonstrated that the battery temperature increases significantly as the charging rate increases for dielectric oil cooling, but the temperature rise remains within the safe thermal limit for the water/glycol coolant. For dielectric cooling, even with the increase of coolant flow rate, the heat transfer coefficient is not increased high enough compared to that of the water/glycol (h = 5976 $W \cdot m^{-2} \cdot K^{-1}$) and reaches h = 696.14 $W \cdot m^{-2} \cdot K^{-1}$ for a fluid velocity of 3 ms^{-1}. Two factors are responsible for reducing the heat transfer coefficient. One factor is low thermal conductivity of the dielectric oil, and another factor is high viscosity. It could be seen that when increasing C-rate greater than 2C, the dielectric cooling is not sufficient in managing the heat load. By comparison, water/glycol shows promising temperature reduction even at the 5C rate due to its higher heat transfer coefficient, resulting from high thermal conductivity and low viscosity. For water/glycol cooling, the temperature is maintained up to 36 °C for 5C. To reduce battery temperature further, mass flow rate has to be increased, which can incur an additional cost, and an extra hardware arrangement is necessary for the cooling system.

Table 6. Predicted battery temperature with various coolants.

C-Rate [C]	Predicted Battery Temperature, [°C] @ Mineral Oil	Predicted Battery Temperature, [°C] @ Water/Glycol [50% + 50%]
0.5	23.10	20.44
1	27.30	21.00
2	41.40	23.60
3	59.00	27.00
4	79.00	31.00
5	101.00	36.00

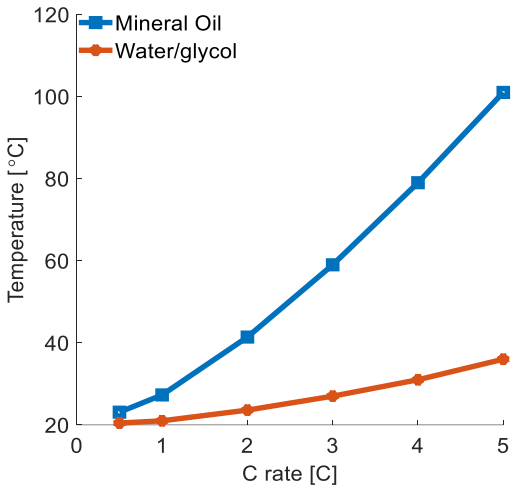

Figure 11. Predicted battery temperature profiles at different C rates.

These results also illustrate that the battery temperature is highly dependent on the choice of coolant. The above analysis indicates that dielectric oil cooling can ensure the battery operation up to 2C, whereas water/glycol can ensure it up to 5C. This is due to the resulting high heat transfer coefficient of the water/glycol. It can be also pointed out that increasing flow rate for water/glycol does not cool the battery sufficiently. In this study, 3 ms^{-1} is considered to be the highest coolant flow velocity.

3.4. Validation of Thermal Performance Analysis under Custom Drive Profile

External factors like the driving scenario also influences battery thermal behavior. When an e-motorbike undergoes an accelerated drive profile, the battery temperature will be changed accordingly. In this section, thermal performance will be analysed under two different custom drive profiles. Figures 12 and 13 show the custom drive profiles and corresponding predicted temperature profiles.

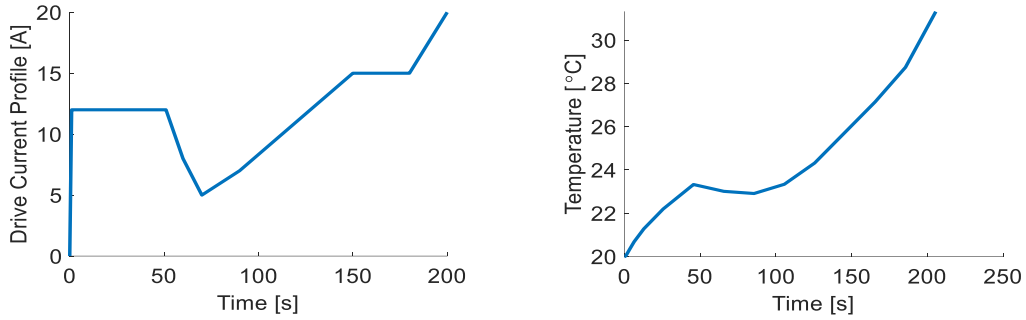

Figure 12. (**a**) First custom drive current profile and corresponding (**b**) predicted temperature profile.

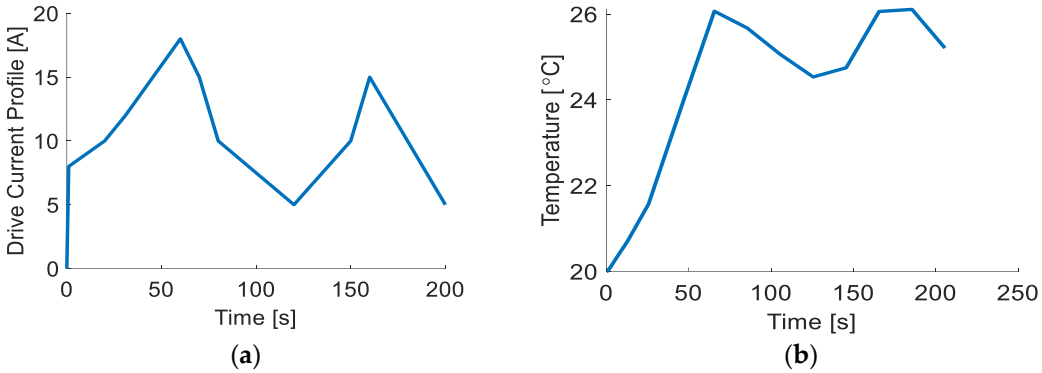

Figure 13. (**a**) Second custom drive current profile and corresponding (**b**) predicted temperature profile.

Overall, the final temperature under the first drive cycle is around 31.31 °C. Temperature rise is observed when the current starts to increase after 90 s. Another observation in the second drive current profile with cyclic variation is that the temperature rises and drops due to increasing and decreasing currents in the drive profiles. These results clearly demonstrate that the thermal management via a liquid cold plate could maintain battery temperature within the safe limit even under different driving scenarios.

To validate the results of the first custom drive profile, further FEA simulations are conducted by feeding the current at 30 s, 60 s, 150 s, and 200 s. The current applied in each cell was 12 A, 8 A, 15 A, and 20 A. The results agree well with the predicted temperature profile from the custom drive profile results illustrated in Figure 12b. The error has been found as 1.76%, 0.76%, 0.86%, and 0.64%, respectively, for the applied currents. The results suggest that the battery temperature is well within the operating range and the error is also within the acceptable level of less than 2%.

3.5. Uncertainity Analysis

In this work, two input parameters were considered that can affect the output battery temperature. The variation in input charging/discharging current can affect the heat generation rate. On the other hand, the variation in coolant flow can affect the overall heat transfer coefficient. To investigate the model's uncertainty, a ±5–10% variation in cell current and heat transfer coefficient for each C rate from 1C to 5C is used to assess how well the model responds to the changes in the input parameters. Table 7 illustrates the results of variation in temperature with ±5% and ±10% variation in the input parameters.

Table 7. Errors in predicted battery temperature with various charging rates and heat transfer coefficients (ambient temperature: 45 °C, coolant: water/glycol and housing material: Cu).

C-Rate [C]	Predicted Battery Temperature, [°C]				Predicted Battery Temperature, [°C] @ 5% Variation in Charging Current + Heat Transfer Coefficient			Predicted Battery Temperature, [°C] @ 10% Variation in Charging Current + Heat Transfer Coefficient		
	Heat Transfer Coefficient [$W \cdot m^{-2} \cdot K^{-1}$]	No Variation	+5% Variation	−5% Variation	Relative Error @ +5% (%)	Relative Error @ −5% (%)	+10% Variation	−10% Variation	Relative Error @ +5% (%)	Relative Error @ −5% (%)
1	2647	21.00	21.10	21.00	0.47	0.00	21.20	20.90	0.95	0.47
2	3432	23.60	23.80	23.40	0.84	0.84	24.00	23.00	1.69	2.54
3	4321	27.00	27.50	26.50	1.85	1.85	28.00	26.00	3.70	3.70
4	5165	31.00	32.00	30.50	3.22	1.61	33.00	29.50	6.45	4.83
5	5976	36.00	37.00	35.00	2.77	2.78	39.00	34.00	8.33	5.55

When the variation that has been added is positive in the input parameters, temperature rise has been observed in both cases. Here, positive variation means a slightly increased charging/discharging current and coolant flow rate and vice versa. This means that the system responds to the input variation and predicted temperature is within the acceptable limit and relative error is also within the error bounds. A similar trend has been observed when the variation of the input used has been negative. Relative error is found high at 5C rate for ±10% variation compared to the results obtained at no variation. To keep the relative error within a reasonable limit, high coolant flow needs to be ensured to tackle the battery temperature rise. It can be pointed out that the model seems robust in terms of thermal performance, indicated by the capability to respond to the changes in the input parameters and a small relative error (3% to 8%) for the variation of ±5% and ±10% charging current and heat transfer coefficient.

3.6. General Discussion

One can argue that metal housing can be problematic due to the risk of causing a short-circuit to the cells. This can be easily eliminated by the choice of appropriate adhesive material such as epoxy/thermal paste. The impact of thermal grease is not studied in this work. In future work, the study of the effect of thermal interface material on the metal housing can be carried out. First, the insulating material such as thermal grease can be a contributing factor to retain internal cell heat. Second, the battery enclosure needs to be protected from direct sunlight exposure, particularly in hot climatic conditions. This can be solved by using a painted, light-coloured battery housing material. From the integration perspective, liquid cold-plate-based cooling requires a pump and additional arrangements, and this involves an additional cost as well. Another concern is leakage, which is a critical safety issue for the battery. This problem can be tackled by adding a substantial grease layer to the battery enclosure material.

In this work, the simulations are focused on managing battery temperature at hot climatic conditions and the reduction of overall battery temperature is the major goal. A battery operating at high ambient conditions might lead to premature battery failure and

early degradation. To avoid these battery failure issues, a novel thermal management strategy has been proposed in this work. Further, with respect to novelty, a new FE thermal model of an e-bike battery has been developed considering various case materials (Al and Cu). In addition, a liquid cooling system has been proposed for an e-bike, which is new in terms of application. To the authors' knowledge, there is no existing work available on the thermal analysis of an e-bike battery, particularly in hot climate conditions.

The battery requirements and pack design for an e-bike could be different from that used in the EVs in a number of ways. The e-bike is better suited for low speed in urban areas and for short trips (range 5–40 miles), whereas the EV is specifically designed for long-distance commuting (city-to-city) at high speed. The proposed e-bike battery pack ideally should be cheaper, lightweight, and compactly designed. The battery temperature can be kept to an optimum level of 28 °C based on the combination of worst-case scenarios, such as 45 °C ambient temperature, battery operating at maximum 5C discharge rate, and coolant temperature at 20 °C, with the combination of Cu casing material and water/glycol coolant. The battery temperature can be further reduced to 20.1 °C by keeping the coolant temperature at 5 °C. However, this comes with an additional cost arising from the chiller needed to maintain a low coolant temperature. An e-bike needs additional cooling only in a harsh ambient temperature of 45 °C and above. Without liquid cooling, the cost can be kept low, which is a promising, environmentally friendly, and cheaper transport option for city dwellers. The proposed design can be lightweight, particularly when the liquid cooling is not needed during the winter, through a modularized battery pack design.

It should also be pointed out that the proposed thermal management was validated using a couple of driving scenarios. However, in the future, an experimental setup would be developed for further validation and implementation of the cooling system in electric bike battery applications.

4. Conclusions

In this study, a detailed numerical simulation that offers an effective solution of battery cooling for electric motorbikes in hot climatic conditions is presented. This cooling solution comes from the combination of battery housing material and coolant flow. The proposed cooling solution depends on high thermal conductivity battery casing material. These findings offer important thermal design guidelines to future e-bike applications. Numerical evaluation suggests that only up to 53 °C is achievable with Cu battery housing material, compared to 55 °C at the maximum discharge rate of 5C. Further reduction is possible with the help of liquid flow cooling configuration and, in this case, with the use of a coolant temperature of 20 °C, battery temperature can be reduced to 28 °C. The analysis also suggests that the proposed cooling system can keep a safe battery temperature up to a 5C discharge rate. Furthermore, the proposed design can maintain a safe battery temperature under different accelerating driving scenarios. Therefore, this cooling system can offer a novel thermal design approach in e-bike applications, where highly conductive battery housing material can be selected together with an appropriate cooling configuration and coolant. This extra layer of thermal design can benefit the power density battery pack design in future e-bike applications while meeting the stringent requirements of battery safety and reliability in hot climatic conditions.

Author Contributions: All authors have equal contribution to prepare and finalise the manuscript. Conceptualization, M.S., T.S., S.B.H., P.K.R., A.A.J., M.A., J.I.C., M.R.A., S.B.A. and J.H.; methodology, M.S., T.S., S.B.H., P.K.R., A.A.J., M.A., J.I.C., M.R.A., S.B.A. and J.H.; software, M.S., T.S., S.B.H., P.K.R. and A.A.J.; validation, M.S., T.S., S.B.H., P.K.R., A.A.J., M.A., J.I.C., M.R.A., S.B.A. and J.H.; formal analysis, M.S., T.S., S.B.H., P.K.R., A.A.J., M.A., J.I.C., M.R.A., S.B.A. and J.H.; investigation, M.S., T.S., S.B.H., P.K.R., A.A.J., M.A., J.I.C., M.R.A., S.B.A. and J.H.; writing—original draft preparation, M.S., T.S., S.B.H., P.K.R., A.A.J.; writing—review and editing, M.S., T.S., S.B.H., P.K.R., A.A.J., M.A., J.I.C., M.R.A., S.B.A. and J.H.; visualization, M.S., T.S., S.B.H., P.K.R., A.A.J., M.A., J.I.C., M.R.A., S.B.A. and J.H.; supervision, M.A., J.I.C., M.R.A., S.B.A. and J.H. All authors have read and agreed to the published version of the manuscript.

Funding: This research received no external funding.

Institutional Review Board Statement: Not applicable.

Informed Consent Statement: Not applicable.

Data Availability Statement: The data presented in this study are available in article.

Acknowledgments: The authors would like to thank University of Warwick for supporting this research work.

Conflicts of Interest: The authors declare no conflict of interest.

References

1. Zhang, J.; Zhang, L.; Sun, F.; Wang, Z. An overview on thermal safety issues of lithium-ion batteries for electric vehicle application. *IEEE Access* **2018**, *6*, 23848–23863. [CrossRef]
2. Kuang, X.; Li, K.; Xie, Y.; Wu, C.; Wang, P.; Wang, X.; Fu, C. Research on control strategy for a battery thermal management system for electric vehicles based on sec-ondary loop cooling. *IEEE Access* **2020**, *8*, 73475–73493. [CrossRef]
3. Sundin, D.W.; Sponholtz, S. Thermal Management of Li-Ion Batteries with Single-Phase Liquid Immersion Cooling. *IEEE Open J. Veh. Technol.* **2020**, *1*, 82–92. [CrossRef]
4. Hu, Z.; He, X.; Restuccia, F.; Yuan, H.; Rein, G. Numerical study of scale effects on self-heating ignition of lithium-ion batteries stored in boxes, shelves and racks. *Appl. Therm. Eng.* **2021**, *190*, 116780. [CrossRef]
5. Behi, H.; Karimi, D.; Jaguemont, J.; Gandoman, F.H.; Kalogiannis, T.; Berecibar, M.; Van Mierlo, J. Novel thermal management methods to improve the performance of the Li-ion batteries in high discharge current applications. *Energy* **2021**, *224*, 120165. [CrossRef]
6. Li, Y.; Yang, J.; Song, J. Design principles and energy system scale analysis technologies of new lithium-ion and alumi-num-ion batteries for sustainable energy electric vehicles. *Renew. Sustain. Energy Rev.* **2017**, *71*, 645–651. [CrossRef]
7. Wang, Q.; Sun, Q.; Ping, P.; Zhao, X.; Sun, J.; Lin, Z. Heat transfer in the dynamic cycling of lithium–titanate batteries. *Int. J. Heat Mass Transf.* **2016**, *93*, 896–905. [CrossRef]
8. Ge, H.; Huang, J.; Zhang, J.; Li, Z. Temperature-adaptive alternating current preheating of lithium-ion batteries with lithium deposition prevention. *J. Electrochem. Soc.* **2015**, *163*, A290. [CrossRef]
9. Liang, J.; Gan, Y.; Li, Y. Investigation on the thermal performance of a battery thermal management system using heat pipe under different ambient temperatures. *Energy Convers. Manag.* **2018**, *155*, 1–9. [CrossRef]
10. Vetter, J.; Novák, P.; Wagner, M.R.; Veit, C.; Möller, K.-C.; Besenhard, J.O.; Winter, M.; Wohlfahrt-Mehrens, M.; Vogler, C.; Hammouche, A. Ageing mechanisms in lithium-ion batteries. *J. Power Sources* **2005**, *147*, 269–281. [CrossRef]
11. Abraham, D.P.; Liu, J.; Chen, C.; Hyung, Y.; Stoll, M.; Elsen, N.; MacLaren, S.; Twesten, R.; Haasch, R.; Sammann, E.; et al. Diagnosis of power fade mechanisms in high-power lithium-ion cells. *J. Power Sources* **2003**, *119*, 511–516. [CrossRef]
12. Spotnitz, R.; Franklin, J. Abuse behavior of high-power, lithium-ion cells. *J. Power Sources* **2003**, *113*, 81–100. [CrossRef]
13. Spotnitz, R.M.; Weaver, J.; Yeduvaka, G.; Doughty, D.H.; Roth, E.P. Simulation of abuse tolerance of lithium-ion bat-tery packs. *J. Power Sources* **2007**, *163*, 1080–1086. [CrossRef]
14. Bandhauer, T.M.; Garimella, S.; Fuller, T.F. A critical review of thermal issues in lithium-ion batteries. *J. Electrochem. Soc.* **2011**, *158*, R1. [CrossRef]
15. Greco, A.; Jiang, X.; Cao, D. An investigation of lithium-ion battery thermal management using paraffin/porous-graphite-matrix composite. *J. Power Sources* **2015**, *278*, 50–68. [CrossRef]
16. Ni, P.; Wang, X. Temperature field and temperature difference of a battery package for a hybrid car. *Case Stud. Therm. Eng.* **2020**, *20*, 100646. [CrossRef]
17. Behi, H.; Karimi, D.; Jaguemont, J.; Gandoman, F.H.; Khaleghi, S.; Van Mierlo, J.; Berecibar, M. Aluminum heat sink assisted air-cooling thermal management system for high current applications in electric vehicles. In Proceedings of the 2020 AEIT International Conference of Electrical and Electronic Technologies for Automotive (AEIT AUTOMOTIVE), Turin, Italy, 18–20 November 2020; pp. 1–6.
18. Akbarzadeh, M.; Kalogiannis, T.; Jaguemont, J.; Jin, L.; Behi, H.; Karimi, D.; Berecibar, M. A comparative study between air cooling and liquid cooling thermal management systems for a high-energy lithium-ion battery module. *Appl. Therm. Eng.* **2021**, *198*, 117503. [CrossRef]
19. Chen, F.; Huang, R.; Wang, C.; Yu, X.; Liu, H.; Wu, Q.; Bhagat, R. Air and PCM cooling for battery thermal management considering battery cycle life. *Appl. Therm. Eng.* **2020**, *173*, 115154. [CrossRef]
20. Lu, M.; Zhang, X.; Ji, J.; Xu, X.; Zhang, Y. Research progress on power battery cooling technology for electric vehicles. *J. Energy Storage* **2020**, *27*, 101155. [CrossRef]
21. Karimi, D.; Khaleghi, S.; Behi, H.; Beheshti, H.; Hosen, M.S.; Akbarzadeh, M.; Berecibar, M. Lithium-ion capacitor lifetime extension through an optimal thermal management system for smart grid applications. *Energies* **2021**, *14*, 2907. [CrossRef]
22. Yu, G.; Zhang, X.; Wang, C.; Zhang, W.; Yang, C. Convective dimensionless method for measurement of heat genera-tion in a lithium thionyl chloride battery. *J. Electrochem. Soc.* **2013**, *160*, A2027. [CrossRef]

23. Meng, F.; Chen, L.; Xie, Z. Numerical simulations and analyses on thermal characteristics of 18650 lithium-ion batteries with natural cooling conditions. *Int. J. Energy Environ.* **2017**, *8*, 43.
24. Wang, D.; Bao, Y.; Shi, J. Online lithium-ion battery internal resistance measurement application in state-of-charge es-timation using the extended kalman filter. *Energies* **2017**, *10*, 1284. [CrossRef]
25. LITHIUM-ION/NNP + HRL Technology. Available online: https://www.imrbatteries.com/content/panasonic_ncr18650b-2.pdf (accessed on 20 May 2022).
26. Yang, N.; Zhang, X.; Li, G.; Hua, D. Assessment of the forced air-cooling performance for cylindrical lithium-ion bat-tery packs: A comparative analysis between aligned and staggered cell arrangements. *Appl. Therm. Eng.* **2015**, *80*, 55–65. [CrossRef]
27. Rao, Z.; Qian, Z.; Kuang, Y.; Li, Y. Thermal performance of liquid cooling based thermal management system for cylin-drical lithium-ion battery module with variable contact surface. *Appl. Therm. Eng.* **2017**, *123*, 1514–1522. [CrossRef]
28. Panchal, S.; Khasow, R.; Dincer, I.; Agelin-Chaab, M.; Fraser, R.; Fowler, M. Thermal design and simulation of mini-channel cold plate for water cooled large sized prismatic lithium-ion battery. *Appl. Therm. Eng.* **2017**, *122*, 80–90. [CrossRef]
29. Kim, G.-H.; Pesaran, A. Battery thermal management design modeling. *World Electr. Veh. J.* **2007**, *1*, 126–133. [CrossRef]
30. Bergman, T.L.; Incropera, F.P.; DeWitt, D.P.; Lavine, A.S. *Fundamentals of Heat and Mass Transfer*; John Wiley & Sons: Hoboken, NJ, USA, 2011.